Int. J. Electrochem. Sci., 12 **(2017)** 10493 – 10510, doi: 10.20964/2017.11.33

International Journal of
ELECTROCHEMICAL
SCIENCE
www.electrochemsci.org

Bioleaching of Chalcopyrite-bornite and Chalcopyrite-pyrite Mixed Ores in The Presence of Moderately Thermophilic Microorganisms

Yulin Huang[1,2], *Yisheng Zhang*[1,2], *Hongbo Zhao*[1,2*], *Yanjun Zhang*[1,2], *Yuming Xiong*[1,2], *Luyuan Zhang*[1,2], *Jun Zhou*[1,2], *Jun Wang*[1,2], *Wenqing Qin*[1,2], *Guanzhou Qiu*[1,2]

[1] School of Minerals Processing & Bioengineering, Central South University, Changsha 410083, Hunan, China
[2] Key Lab of Bio-hydrometallurgy of Ministry of Education, Changsha 410083, Hunan, PR China
[*]E-mail: zhbalexander@csu.edu.cn; alexandercsu@126.com

Received: 21 July 2017 / *Accepted:* 11 September 2017 / *Published:* 12 October 2017

In this work, bioleaching of chalcopyrite-pyrite and chalcopyrite-bornite mixed ores in the presence of moderately thermophilic microorganisms (*A.caldus*, *L.ferriphilum* and mixed culture) were carried out. Bioleaching results showed that bioleaching behaviors of chalcopyrite-pyrite and chalcopyrite-bornite mixed ores in the presence of these moderately thermophilic microorganisms were all in accordance with the proposed optimum redox potential theory. Results showed that high copper extraction was obtained in different bioleaching systems if the redox potential was between E_L to E_H. Real-time PCR technique was used to analyze the change of percentages of *A.caldus* and *L.ferriphilum* during bioleaching by mixed culture consisting of *A.caldus* and *L.ferriphilum*. Results showed that the change rules were similar between bioleaching system of sole chalcopyrite and two kinds mixed ores, indicating that the chemical factor instead of biological factor should be the main cause for the high copper extraction of chalcopyrite-pyrite and chalcopyrite-bornite mixed ores.

Keywords: Chalcopyrite; Pyrite; Bornite; Redox potential; Real-time PCR

1. INTRODUCTION

Global ore reserves are declining rapidly due to the large industrial demand [1]. However, this difficulty can be overcome by utilizing the huge reserves of refractory ores [2]. As a specialized bio-hydrometallurgy process, bioleaching is a promising process involving the mobilization of metals from ores in the presence of microorganisms [3]. Bio-hydrometallurgy treatment of low-grade copper ore in the case of eco-friendly and low cost, which will make it an important technique for the metallurgical industry [4].

As the most important copper ore, chalcopyrite is recalcitrant to bio-hydrometallurgical processing for its slow rate of dissolution [5]. Many factors influence the dissolution rate of chalcopyrite, including temperature, pH, microorganisms and the oxidation-reduction potential (ORP), etc [6]. Previous studies have shown that the bioleaching of chalcopyrite conforms to the optimum redox potential theory, which will be explained below [7, 8]. However, chalcopyrite is usually associated with a variety of minerals in nature, including pyrite, bornite and other sulfide minerals. These associated minerals exist in the bio-hydrometallurgy system of chalcopyrite, which cannot be neglected in the process of bioleaching of chalcopyrite.

Pyrite (FeS_2) is the most common type of associated sulfide minerals in chalcopyrite. Many studies have shown that pyrite can significantly promote the dissolution of chalcopyrite in the ferric sulfate leaching system, and accordingly developed a process called Galvanox^{TM} for the treatment of chalcopyrite [9-12]. The catalytic effect of pyrite on chalcopyrite is widely considered to be the primary battery effect (Galvanic effect). In the primary battery composed of pyrite and chalcopyrite, pyrite acts as a cathode for its higher electrostatic potential, in contrast, chalcopyrite acts as an anode. The direct oxidation reaction of chalcopyrite is enhanced by the galvanic effect. However, extensive studies have shown that low potential contributes to the dissolution of chalcopyrite. The reason is that chalcopyrite can be reduced to a secondary copper-sulfur compound such as chalcocite (Cu_2S) at a lower potential, and the direct oxidation of chalcopyrite at a higher potential easily leads to surface passivation [13-16]. Thus, the effect of pyrite on chalcopyrite bioleaching system need to be further studied.

Bornite (Cu_5FeS_4) is a sort of widespread Cu-bearing sulfide ore which is usually associated with chalcopyrite [17]. Some scholars deem that chalcopyrite is first converted to bornite at the early stage of bioleaching, and this step is a rate-limiting step for the dissolution of the chalcopyrite [18-21]. Acres et al. [22] found that in the leaching system of chalcopyrite, bornite reduced the oxidation rate of chalcopyrite, which inhibited the dissolution of chalcopyrite.

Bioleaching processes employ microorganisms that are dominated by acidophilic, autotrophic iron- or sulfur- oxidizing prokaryotes [23]. The microorganisms of bioleaching have been categorized using a number of different criteria, and classification by growth temperature is one of the most common methods. According to this method, microorganisms are divided into three kinds, including mesophiles, moderately thermophilic microorganisms and extremely thermophiles. The optimum growth temperature of the three kinds microorganisms are about 40 ^{o}C, 40-60 ^{o}C and 60 ^{o}C, respectively [24].

In recent years, the focus has shifted from mesophilic microorganisms to moderately thermophilic or thermophilic microorganisms [25]. The reason is that bioleaching in the presence of mesophiles needs low temperature (<40 ^{o}C), which will lead to rapid surface passivation of the ores. In addition, extremely thermophiles are sensitive to high pulp concentration. Thus, the moderately thermophilic microorganisms have been widely applied in industry. In addition, many studies have shown that microbial interactions are widespread in bioleaching systems, and that mixed cultures are more robust and more efficient than pure cultures on oxidizing minerals [26].

On the one hand, as the important copper-bearing ore, chalcopyrite usually exists in nature associated with pyrite and bornite, so the ores we processed were usually mixed type. Hence, it is

important to understand the bioleaching behaviors of mixed ores and the main causes of differences of bioleaching behaviors between single chalcopyrite and mixed ores. On the other hand, moderately thermophilic microorganisms are more suitable for bioleaching than mesophiles and extremely thermophiles. According to the above, in this paper, two representative moderately thermophilic microorganisms, *Acidithiobacillus caldus* (*A. caldus*) and *Leptospirillum ferriphilum* (*L. ferriphilum*), was selected to build the corresponding bio-hydrometallurgical systems. This work mainly used XRD analysis, XPS analysis, redox potential analysis, electrochemical analysis, solution compositions analysis and real-time PCR technique to explore whether biological factors or chemical factors are the main factors causing the different bioleaching behaviors.

2. EXPERIMENTAL

2.1. Materials and electrodes

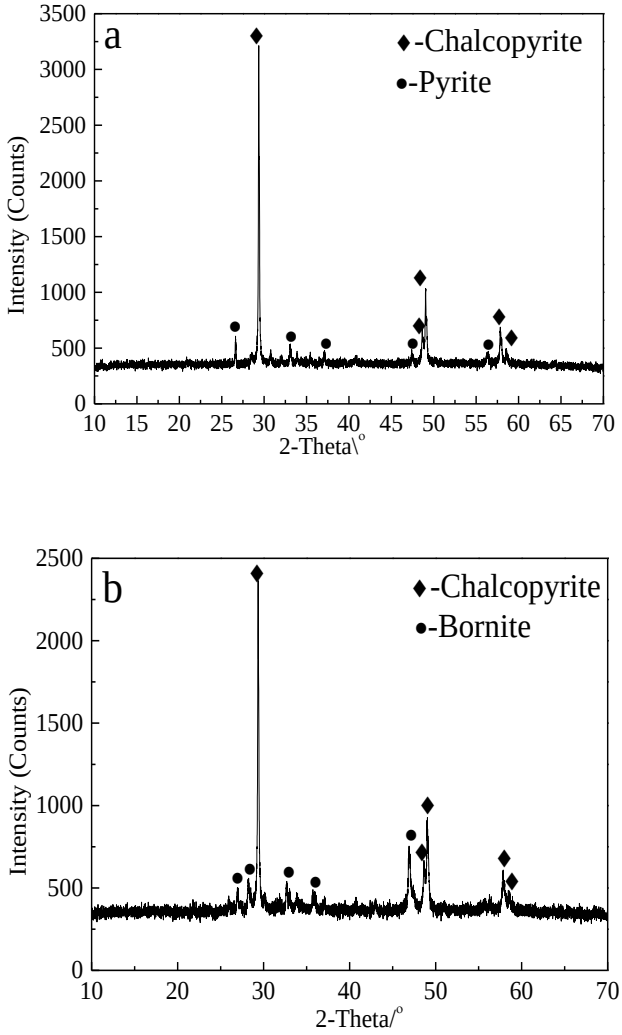

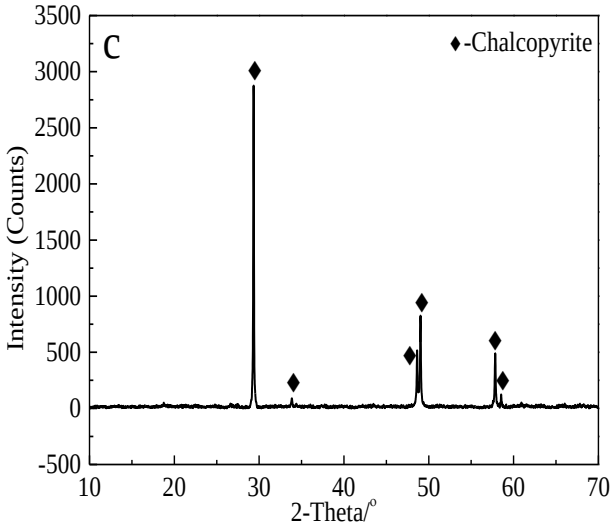

Figure 1. The XRD analysis of chosen mixed type ore: (a) chalcopyrite-pyrite (b) chalcopyrite-bornite (c) chalcopyrite.

The chalcopyrite-pyrite mixed type ore and chalcopyrite-bornite mixed type ore samples were obtained from Daye Mine of Hubei Province of China and Meizhou Mine of Guangdong province of China, respectively. X-ray diffraction (XRD) (Fig.1 (a) and (b)) indicated that the former mainly contained chalcopyrite and pyrite, the latter mainly contained chalcopyrite and bornite, and both of them did not contain other obvious impurities.

The pure chalcopyrite sample was obtained from geological museum of Hunan Province of China. X-ray diffraction (XRD) (Fig.1 (c)) indicated that the samples mainly contained chalcopyrite. Ore samples were all ground and sieved to less than 0.074 mm before used for bioleaching experiments and analysis. The chemical elements analysis of minerals samples showed that chalcopyrite sample mainly contained 34.14% Cu, 31.52% Fe and 33.12% S (wt%), chalcopyrite-pyrite sample mainly contained 24.28% Cu, 34.41% Fe and 33.49% S (wt%) and chalcopyrite-bornite sample mainly contained 40.23% Cu, 24.00% Fe and 32.53% S (wt%).

The electrodes used in electrochemical tests were Carbon Paste Electroactive Electrodes (CPEE). The quality of each electrode was 1 g, including 0.7 g corresponding mineral samples (with size -0.038 mm), 0.2 g graphite and 0.1 g solid paraffin. The first step, these three materials were mixed evenly. The second step, the mixture was heated until paraffin was thawed. The third step, the mixture was transferred into a tablet model immediately, tableted under the compressing pressure of 500 kg/cm^2. The last step, the formed tablet was taken out and dried in the open air for one hour. Then, the corresponding electrodes were obtained. These electrodes were shaped like round coins, their diameters were 1.5 cm and thicknesses were about 0.5 cm. In the electrochemical tests, the contact surface area between the electrode and the solution was 1 cm^2, and the electrodes were polished with 600-grit silicon carbide paper to keep the smooth surface. During every single test, the electrodes were rinsed with distilled water.

2.2. Microorganisms

In this paper, the selected microorganisms are moderately thermophilic microorganisms, including *Acidithiobacillus caldus* (*A. caldus*) (CCTC AB 206240) and *Leptospirillum ferriphilum* (*L. ferriphilum*) (CCTC AB 206239), which were initially obtained from the Key Lab of Bio-hydrometallurgy of Ministry of Education, Central South University, Changsha, China. Microorganisms were cultured in 250 mL erlenmeyer flasks. Firstly, added 100 mL of the basic salt solution medium after high temperature sterilization in every 250 mL erlenmeyer flask. The medium consists of $(NH_4)_2SO_4$ (3.0g/L), KCl (0.1 g/L), K_2HPO_4 (0.5g/L), $MgSO_4 \cdot 7H_2O$ (0.5 g/L), $Ca(NO_3)_2$ (0.01 g/L). Secondly, 10g/L sublimed sulfur was added as an energy source in the basic salt solution medium of *A. caldus*, 44.7g/L $FeSO_4 \cdot 7H_2O$ was added as an energy source in the basic salt solution medium of *L. ferriphilum*. Thirdly, these microorganisms were cultured at 170 rpm, 45 ^oC and pH of 1.70. When the microorganisms grew to logarithmic phase and the cell concentration exceeded 1.0×10^7 cells/mL, the microorganisms were filtered and centrifuged to collect the concentrated microorganism solution as the test strain of bioleaching.

2.3. Bioleaching experiments

The stirred bioleaching test was carried out. Firstly, 3L basic salt solution medium, which had been mentioned above, was added into 5L beaker. Then, added 15g of the corresponding mineral sample (-0.074mm), respectively. Thirdly, added 5mL of the corresponding concentrated microorganism solution to ensure that the initial bacterium concentration in the leaching system was greater than 1.0×10^7 cells/mL, respectively. Finally, adjusted the initial pH of the solution to 1.70 and placed it in a thermostat water bath at a temperature of 45 ^oC and with a stirring speed of 300 rpm.

During the leaching process, dilute sulfuric acid was used to continuously adjust the pH of solution at 1.70. The pH value was monitored with a pH meter (PHSJ-4A). The concentration of Fe^{2+} in solution was analyzed by dichromate titration. The metal ion concentration of the leaching system was measured by using an Inductively Coupled Plasma-Atomic Emission Spectrometer (ICP-AES) model of America Baird Co. PS-6. Oxidation-Reduction Potential (ORP) was measured by using an ORP meter (BPP-922), with saturated Ag/AgCl as the reference electrode. Using the optical microscope (CX3), the microbial concentration of leaching system was analyzed by blood cell counting plate. Distilled water was used to replenish moisture due to evaporation during the whole process.

After leaching, the solution was filtered through neutral filter paper and rinsed with distilled water at pH 1.70 for 3 times. The residues was transferred to a vacuum oven (DZF-6050), dried at 40 ^oC for 12 h. Then the dry residues were correspondingly detected.

2.4. Analytic techniques

2.4.1. X-Ray Powder Diffractometer, (XRD)

The XRD analysis of mineral samples was carried out using a Bruker D8 Advance X-Ray diffractometer (Cu Kα, is1.5406Å). The operating voltage was 40 kV, the operating current was 40 mA,

the step and step time were 0.004° and 28.5 s, respectively, and the operating temperature was 25 °C.

2.4.2. X-ray Photoelectron Spectroscopy, (XPS)

The XPS analysis of mineral samples was carried out using the equipment (ESCALAB 250Xi) produced by Thermo Fisher Scientific Inc. The equipment used a monochromatic Al Kα X-ray excitation source (1486.6 eV). Its power was 200 W, degree of vacuum was less than 1×10^{-9} mbar, pass energy and step were 20 eV and 0.2 eV, respectively. Calibration was performed using C 1s with binding energy of 284.8 eV. S 2p contains S $2p_{3/2}$ and S $2p_{1/2}$, which was double-peak. Thus it was fitted using the analysis software Avantage 5.52. When fitting, the Gaussian-Lorentzian line (SGL) function, with a weight of 30% Lorentzian and 70% Gaussian, was used, the ratio of $2p_{3/2}$ and $2p_{1/2}$ peak was 2:1, the spacing of binding energy was 1.2 eV, and the Shirley method was used to deduct the background [27].

2.4.3. Electrochemical analysis

The electrochemical analysis was carried out using a potentiostat (Princeton Model 283, EG&G of Princeton Applied Research) and a personal computer in a special reactor (a conventional three-electrode system). This reactor was composed of the counter electrode, reference electrode and the working electrode, they were made of two wired graphite, an Ag/AgCl (3.0 M KCl) electrode and corresponding CPEE, respectively. The 9K medium (pH = 1.75) and the nitrogen atmosphere were set up in the reactor. The electrode potential was stabilized for 10 minutes before full scan. The Ag/AgCl (3.0 M KCl) electrode was the reference electrode.

Different potentials were used for potentiostatic tests which lasted for 240 seconds. A sweep rate of 20 mV/s was used for CV measurements. Both positive and negative scan were started from the open circuit potential 200 mV. For positive scan, the switching potential of the forward and reverse scan were 800 mV and -800 mV, respectively. For negative scan, the opposite is true.

2.4.4. Real-time PCR analysis

Table 1. Primer and the corresponding sequence.

Target strain	GenBank NO.	Primer				Product length
		Name	Length	Sequences(5'-3')	Tm/℃	
YSK	EF613030	L-F	18	GAAAACACTTGAGGACGG	55.02	168bp
		L-R	18	CGGATAAAACGGTTGAAT	50.47	
S1	NR103158	Ac-F	18	TGCGGCTCGACTTCTCAC	59.58	150bp
		Ac-R	18	GGGCATAGCGATCAAACG	57.30	

Lixivium was periodically leached from the bioleaching systems, then it was filtrated to collect microorganisms. The genomic DNA of the collected microorganisms was extracted using the

TIANamp Microorganisms DNA kit technique. Real-time PCR primers were synthesized using well-designed sequences of our laboratory by Sangon Biotech (Shanghai) Company. The primers were specific for different genes of different microorganisms. The primer synthesis sequences were shown in Table 1.

In order to detect whether synthetic specific primers can bind to the target gene specifically, 50 μL of the convention PCR reaction system was carried out to conduct the specific amplification of genomic DNA and primers. The composition of the conventional PCR amplification system (50μL) was shown in Table 2. Result showed that the primers had high specificity.

Table 2. The conventional PCR amplification system.

The conventional PCR amplification system (50μL)	
2∗Master mix	25 μL
Forward primer	1 μL
Reverse primer	1 μL
Template DNA	2 μL
DdH_2O	21 μL

The pure genomic DNA was amplified by the conventional PCR. The concentration and purity of the amplified product were determined using spectrophotometer. The PCR amplified product of pure DNA was diluted to 10^{-3}, 10^{-4}, 10^{-5}, 10^{-6}, 10^{-7} times of its original concentration using the tenfold serial dilution method. Then, the real-time PCR reactions of these diluted samples and the original sample were carried out. Before the Real-time PCR reaction, the monochromatic, fluorescence-based real-time PCR instrument (MyiQ^{TM}) was preheated for 30 minutes. The analysis software Optical System (Version 1.0) was set 96 blank boards for samples. As shown in Table 3, the reaction reagents were added to 96 blank boards in turn, then these boards were covered closely by an optical film. This operation avoided light as much as possible.

The data were analyzed by Optical System (Version 1.0) software. The specificity of the reaction judged according to the dissolution curves. The Ct value of the fluorescence curve and the standard curve were used to quantify the reaction specificity.

Table 3. The conventional PCR amplification system**.**

The conventional real-time PCR amplification system（25 μL）	
2∗SYBRR Green timing and quantitative	6 μL
Forward primer	0.5 μL
Reverse primer	0.5 μL
Template DNA	2 μL
ddH_2O	9.5 μL
PCR hybrid system	6.5 μL

3. RESULTS AND DISCUSSION

3.1 The optimum redox potential theory

The chalcopyrite bioleaching process involves a series of complex redox reactions, which will change due to changes in solution composition. Fe^{3+} is the most important oxidant of chalcopyrite-ferric sulfate leaching system and chalcopyrite bio-hydrometallurgy system [28-30]. The solution potential is considered to be the determining factor in the chalcopyrite-ferric sulfate leaching system [31, 32]. Similarly, the solution potential is also the determinant of the chalcopyrite biohydrometallurgy system. Many studies have shown that, the passivation of chalcopyrite occurred quickly if the initial solution potential was too high, only when the potential of the solution was controlled within a suitable range, can we obtain a higher extraction rate of Cu [15, 33-36]. Petersen and Dixon [36] proposed that the higher solution potential was not conducive to the bioleaching of chalcopyrite and the lower solution potential was favorable for the leaching of chalcopyrite. When the solution potential exceeded a critical value (Fe^{3+}/Fe^{2+} is 1), the leaching process was almost stagnant. Ahmadi et al. [37] designed an electrochemical reactor and used for bioleaching of chalcopyrite concentrates, they found that when the solution potential was between 400-425 mV (vs. Ag/AgCl), the chalcopyrite can be leached efficiently. Many scholars believed that chalcopyrite can be highly leached in a suitable solution potential range because chalcopyrite can be converted to chalcocite (Cu_2S) under this condition. Then, Cu_2S was oxidized and dissolved rapidly to obtain a higher Cu leaching rate [13-16]. This process can be expressed by the reaction formulas (1) - (2) [1]**.**

$$CuFeS_2 + 3Cu^{2+} + 4e^- \rightarrow 2Cu_2S + Fe^{2+} \quad (1)$$

$$2Cu_2S \rightarrow 4Cu^{2+} + 2S^0 + 8e^- \quad (2)$$

For the reaction formula (1), the Gibbs free energy (G) was calculated as shown in equation (3).

$$\Delta G = \Delta G^0 + RT \ln \frac{\left(aFe^{2+}\right)}{\left(aCu^{2+}\right)^3} = -nEF \quad (3)$$

Thereinto, G was the Gibbs free energy, R was the gas constant (8.314 $Jmol^{-1}K^{-1}$), T was the absolute temperature (318 K), F was the Faraday constant (96485 $Cmol^{-1}$), n was the charge transfer number, E was reaction potential.

The thermodynamic formula of the above chemical reaction can be further established by combining the Nernst equation, as shown in equation (4).

$$E = E^0 + \frac{RT}{F} \ln \frac{\left[Fe^{3+}\right]}{\left[Fe^{2+}\right]} \quad (4)$$

Based on the above equation, the highest critical potential (defined as E_H) on the thermodynamics of the chemical reaction (1) that chalcopyrite was reduced to Cu_2S can be calculated by this formula (5):

$$E_H = 482 + 47.3 \lg\left(aCu^{2+}\right) - 15.77 \lg\left(aFe^{2+}\right) / mV \quad (5)$$

In the presence of Cu^{2+}, chalcopyrite can be converted to Cu_2S only when the solution potential was below the highest critical potential E_H. From equation (5) we can see that the highest

critical potential E_H was the equation containing the Cu^{2+} and Fe^{2+} concentration parameters. Thus, E_H was affected by the concentration of Cu^{2+} and Fe^{2+} in the solution.

The thermodynamic equation for the chemical reaction (2) that the intermediate product Cu_2S was further oxidized and dissolved was shown in this equation: (6).

$$\Delta G = \Delta G^0 + RT \ln\left(aCu^{2+}\right)^4 = -nEF \qquad (6)$$

The lowest critical potential (defined as E_L) on the thermodynamics of the chemical reaction (2) can be calculated by this formula (7):

$$E_L = 401 + 29.5 \lg\left(aCu^{2+}\right) / mV \qquad (7)$$

When the solution potential was higher than the lowest critical potential (E_L), the intermediate product Cu_2S can be continuously oxidized and dissolved. From equation (4-7) we can see that the lowest critical potential E_L was the equation containing the Cu^{2+} concentration parameter. Thus, E_L was affected by the concentration of Cu^{2+} in the solution.

In summary, the conversion from chalcopyrite to intermediate product Cu_2S and the further oxidation and dissolution of Cu_2S were controlled by the solution potential, and the critical potentials for the above phase conversions were affected by the concentration of the solution, especially the concentration of Cu^{2+}. In addition, the thermodynamic equation of the chemical reaction shows that the coefficient (slope) of the critical potential equation was affected by the temperature, and the intercept of the equation was not affected by the temperature. Therefore, chalcopyrite can be converted to intermediate product Cu_2S theoretically when the solution potential was in a suitable range (E_L-E_H). Then, Cu_2S was further oxidized and dissolved, thereby strengthening the dissolution process of chalcopyrite.

3.2 Bioleaching system of chalcopyrite-pyrite mixed type ore

Fig. 2 shows that the dissolution process of the chalcopyrite conformed to the optimum potential equation (equations (5) and (7)) in this leaching system of chalcopyrite-pyrite mixed type ore in the presence of moderately thermophilic microorganisms *A. caldus* and *L. ferriphilum*, respectively.

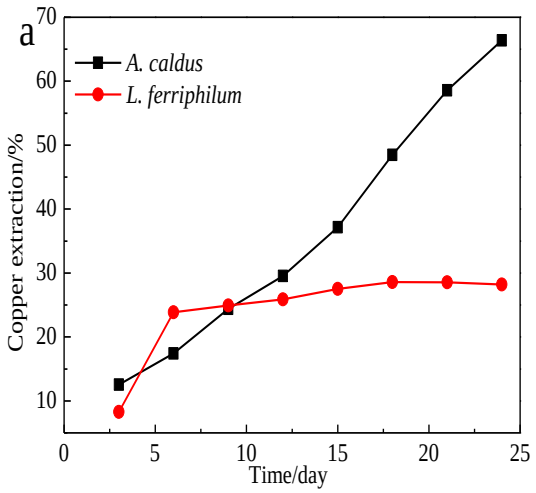

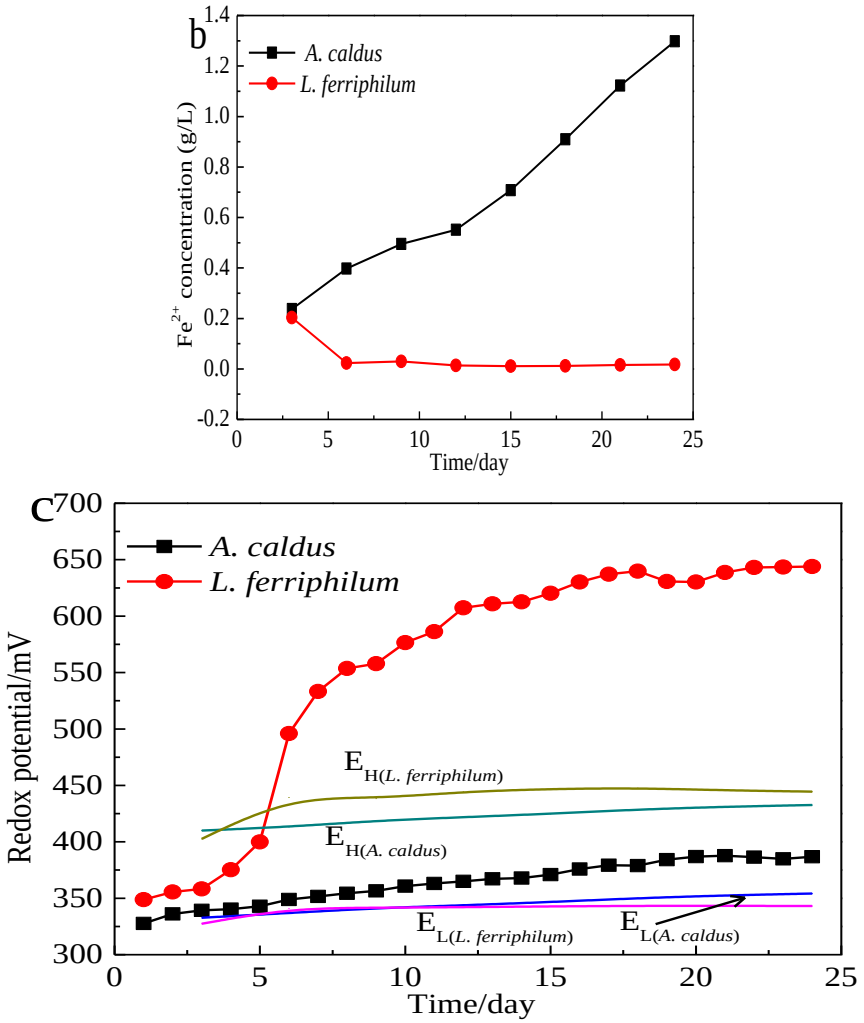

Figure 2. Bioleaching of chalcopyrite-pyrite mixed type ore by moderately thermophilic microorganisms: (a) Copper extraction; (b) Fe^{2+} concentration; (c) Redox potential

Fig. 2(a) and Fig. 2(c) show that the copper extraction in *A. caldus* bioleaching system was higher than that in *L. ferriphilum* bioleaching system, for the redox potential of the former was between E_L and E_H. The results further proved that the optimum redox potential theory and the proposed mechanism of pyrite on chalcopyrite bioleaching were reliable.

Then, experiments were carried out using mixed moderately thermophilic microorganisms (*A. caldus* and *L. ferriphilum*) to leach chalcopyrite and chalcopyrite-pyrite mixed type ore, respectively. And real-time PCR was used to analyze the ratio of *A. caldus* and *L. ferriphilum* in these two leaching systems.

Fig. 3(a) shows the change rule of the ratio of *A. caldus* and *L. ferriphilum* in the leaching process of chalcopyrite in presence of mixed cultures (*A. caldus* and *L. ferriphilum*). The initial ratio of *A. caldus* and *L. ferriphilum* was 1: 1. In the early stage of leaching, *L. ferriphilum* was the dominant species, and *A. caldus* was the dominant species in the late stage of leaching. Fig. 3(b) shows that, similar results can be obtained from the chalcopyrite-pyrite mixed type ore leaching system in the presence of mixed cultures (*A. caldus* and *L. ferriphilum*). Fig. 2(b) shows that, the amount of Fe^{2+} was sufficient in the early stage of leaching system, which was beneficial to the rapid growth of *L.*

ferriphilum, but at the late stage of leaching, the concentration of Fe^{2+} in the leaching system was very low, which was not conducive to the growth of *L. ferriphilum*. The change rules of microbial proportion of leaching system in the two ore leaching systems were similar, which showed that the effect of pyrite on the bioleaching of chalcopyrite was mainly due to chemical factors, rather than biological factors.

Actually, some researchers had studied the role of pyrite in hydrometallurgical process of chalcopyrite and proposed that the galvanic effects enhanced chalcopyrite dissolution, and a process known as Galvanox^{TM} had been developed to extract chalcopyrite [9-12]. However, our previous work found that the addition of pyrite mainly controlled the redox potential at an optimum range in which the passivation layer of polysulfide on the mineral surface was inhibited, thus resulting in higher copper extraction [38, 39]. It was consistent with the obtained results of this work.

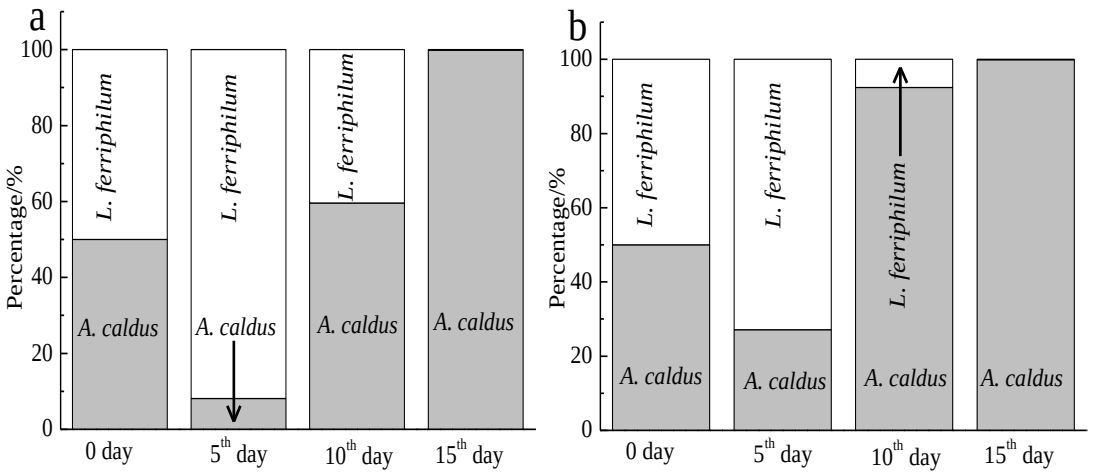

Figure 3. Percentages of *A. caldus* and *L. ferriphilum* during bioleaching: (a) Chalcopyrite; (b) Chalcopyrite-pyrite mixed type ore.

3.3 Bioleaching system of chalcopyrite–bornite mixed type ore

Fig. 4 shows that the dissolution process of the chalcopyrite conformed to the optimum potential equation (equations (5) and (7)) in this leaching system of chalcopyrite-bornite mixed type ore in the presence of moderately thermophilic microorganisms *A. caldus* and *L. ferriphilum*, respectively. Fig. 4(a) and Fig. 4(c) show that high copper extraction rate can be obtained in both *A. caldus* bioleaching system and *L. ferriphilum* bioleaching system, for their redox potentials can be maintained at the optimum potential interval for a long time. However, the final copper extraction in *A. caldus* bioleaching system was higher than that in *L. ferriphilum* bioleaching system, for the redox potential of the former was always between E_L and E_H.

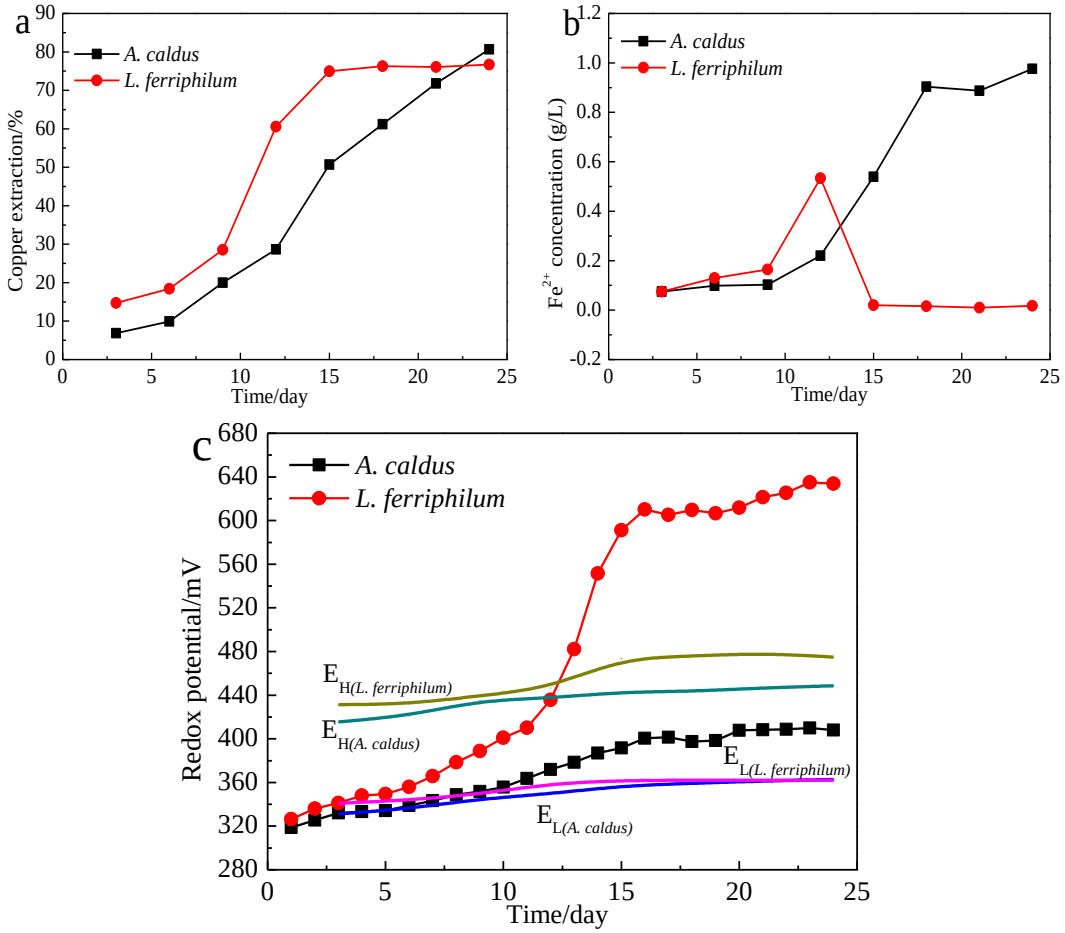

Figure 4. Bioleaching of chalcopyrite-bornite mixed type ore by moderately thermophilic microorganisms: (a) Copper extraction; (b) Fe^{2+} concentration; (c) Redox potential.

The samples of chalcopyrite-bornite mixed type ore leaching residues after leaching for ten days in the presence of *L. ferriphilum* were further analyzed by XRD and XPS analysis. At this time, the solution potential was in the optimal potential interval, so, the samples were representative. Fig. 5 shows that, after leaching for ten days, bornite had been dissolved completely, chalcopyrite was mainly remained in the system and accompanied by the formation of elemental sulfur. The results of XPS analysis of leaching residues samples are shown in Fig. 6. The binding energy and half-width values of the S $2p_{3/2}$ peak after the XPS fitting are shown in Table 4. According to previous publications [30], it was found that the S-containing materials on the surface of residues were mainly S^{2-}, S_2^{2-}, S^0 and SO_4^{2-}, the proportion of them reached 48.68%, 16.02%, 18.45% and 16.85%, respectively. No obvious Sn^{2-} was discovered in the leaching system. And a large amount of S^0 did not significantly impede the dissolution of chalcopyrite.

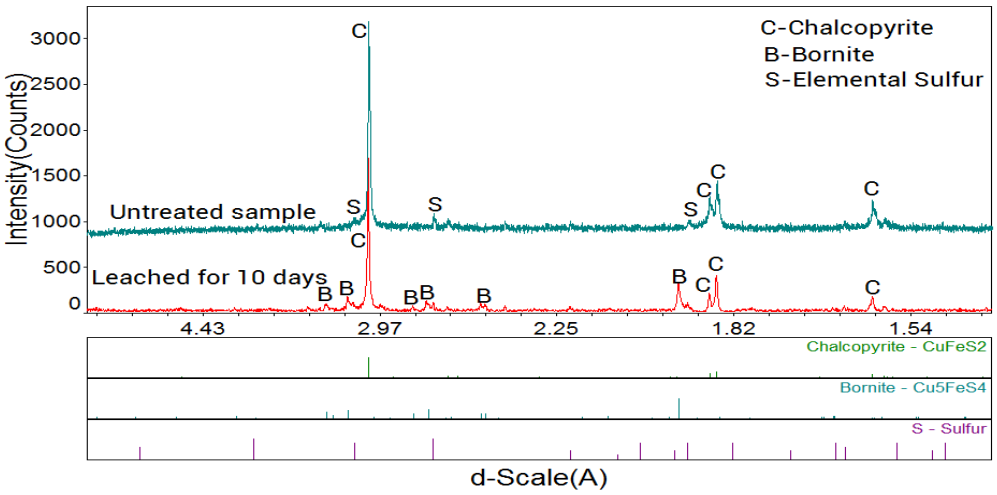

Figure 5. XRD analysis of chalcopyrite-bornite mixed type ore leached by *L. ferriphilum* for 10 days.

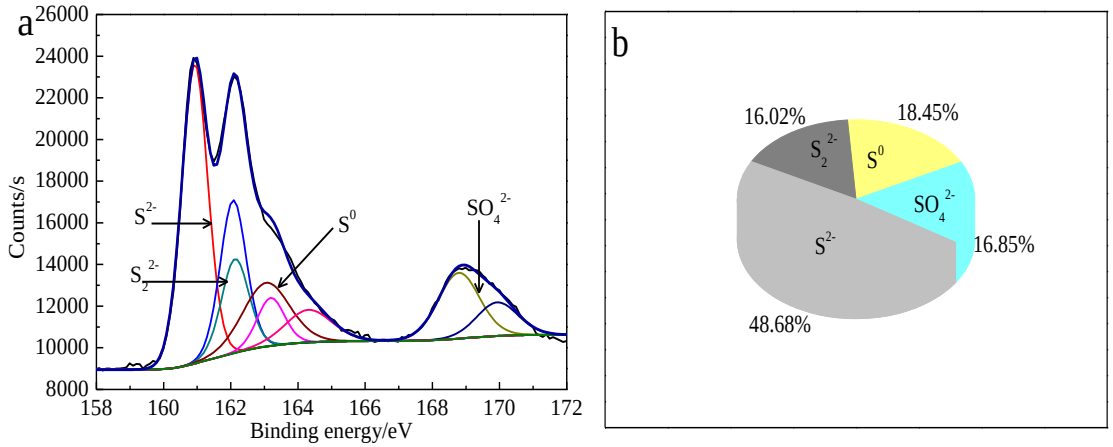

Figure 6. XPS analysis of chalcopyrite-bornite mixed type ore leached by *L. ferriphilum* for 10 days: (a) S 2p spectra; (b) Distribution of sulfur species.

Table 4. Binding energy and FWHM value for XPS spectra of S 2p3/2 peaks of chalcopyrite-bornite mixed type ore leached leached by L. ferriphilum for 10 days.

Time/day	Peak 1		Peak 2		Peak 3		Peak 4	
	B.E. (eV)	FWHM/ eV	B.E. (eV)	FWHM/ eV	B.E. (eV)	FWHM/ eV	B.E. (eV)	FWHM/ eV
10	161.0	0.9	162.2	0.9	163.1	1.7	168.8	1.4

Thus, the results further demonstrated that bornite can control the solution potential of the mixed ore bioleaching system for a long time in a suitable range for chalcopyrite dissolution (equations (5) and (7)). At this point the chalcopyrite can be converted into intermediate product Cu_2S, it inhibited the production of passivation material Sn^{2-}, then the dissolution of chalcopyrite was promoted. The results further proved that the optimum redox potential theory and the proposed mechanism of bornite on chalcopyrite bioleaching were reliable.

Then, experiments were carried out using mixed moderately thermophilic microorganisms (*A. caldus* and *L. ferriphilum*) to leach chalcopyrite and chalcopyrite-bornite mixed type ore, respectively. And real-time PCR was used to analyze the ratio of *A. caldus* and *L. ferriphilum* in these two leaching systems.

Fig. 7 (a) shows the change rule of the ratio of *A. caldus* and *L. ferriphilum* in the leaching process of chalcopyrite in the presence of mixed cultures (*A. caldus* and *L. ferriphilum*). The initial ratio of *A. caldus* and *L. ferriphilum* was 1: 1. In the early stage of leaching, *L. ferriphilum* was the dominant species, and *A. caldus* was the dominant species in the late stage of leaching. Fig. 7(b) shows that, similar results can be obtained from the chalcopyrite-pyrite mixed type ore leaching system in the presence of mixed cultures (*A. caldus* and *L. ferriphilum*). This was due to the sufficient amount of Fe^{2+} in the early stage of leaching system, which was beneficial to the rapid growth of *L. ferriphilum*, but at the late stage of leaching, the concentration of Fe^{2+} in the leaching system was very low, which was not conducive to the growth of *L. ferriphilum*. The change rules of microbial proportion of leaching system in the two ore leaching systems were similar, which showed that the effect of pyrite on the bioleaching of chalcopyrite was mainly due to chemical factors, rather than biological factors.

Some researchers [18-21, 40] had proposed that chalcopyrite can be reduced to bornite at the initial stage and this first step was also a rate-limiting step in the whole bioleaching process. Acres et al. [22] found that bornite decreased the oxidation rate of chalcopyrite and inhibited chalcopyrite dissolution in hydrochloric acid leaching process. Our previous work proposed that a synergistic effect existed between chalcopyrite and bornite during bioleaching, the presence of bornite promoted chalcopyrite bioleaching mainly through controlling the redox potential at an appropriate range [38, 41]. That was also in accordance with the obtained results of this work.

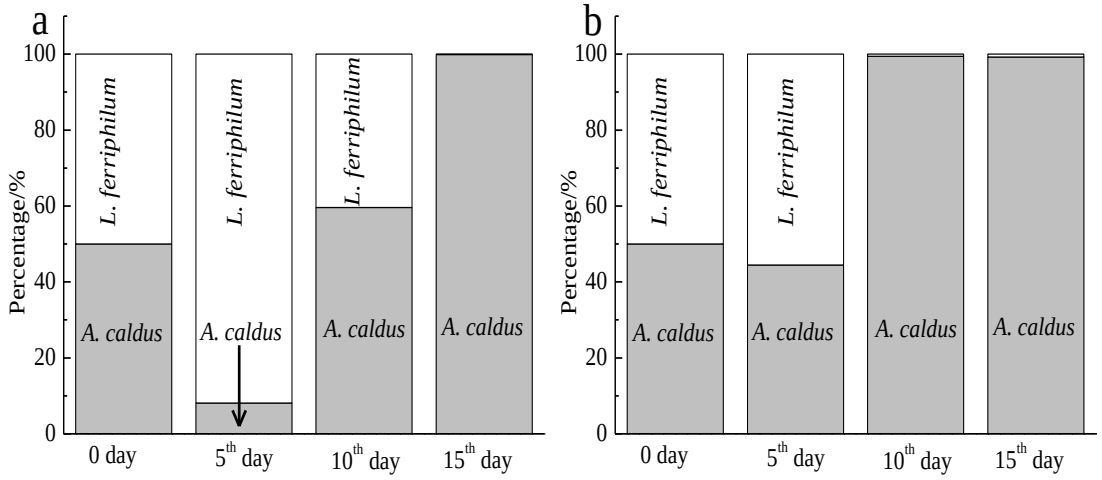

Figure 7. Percentages of *A. caldus* and *L. ferriphilum* during bioleaching: (a) Chalcopyrite; (b) Chalcopyrite-bornite mixed type ore.

3.4 Electrochemical analysis

Fig. 8 shows the cyclic voltammograms of chalcopyrite, bornite, pyrite, chalcopyrite-bornite

mixed ore and chalcopyrite-pyrite mixed ore electrode. Fig. 8a and Fig. 8b both indicate that eight peaks had appeared on the cyclic voltammograms of chalcopyrite. According to previous studies, each peak corresponded to one or more specific chemical reactions which were listed as follows [17, 42].

Peak 1:

$$Cu^{2+} + S^0 + 2e^- \rightarrow CuS \quad (8)$$

$$Cu^{2+} + CuS + 2e^- \rightarrow Cu_2S \quad (9)$$

$$2CuS + 2H^+ + 2e^- \rightarrow Cu_2S + H_2S \quad (10)$$

$$Cu^{2+} + 2e^- \rightarrow Cu^0 \quad (11)$$

$$CuFeS_2 + 3Cu^{2+} + 4e^- \rightarrow Cu_5FeS_4 + Fe^{2+} \quad (12)$$

$$CuFeS_2 + 3Cu^{2+} + 4e^- \rightarrow 2Cu_2S + Fe^{2+} \quad (13)$$

$$9CuFeS_2 + 4H^+ + 2e^- \rightarrow Cu_9Fe_8S_{16} + 2H_2S + Fe^{2+} \quad (14)$$

$$5CuFeS_2 + 12H^+ + 4e^- \rightarrow Cu_5FeS_4 + 6H_2S + 4Fe^{2+} \quad (15)$$

Peak 2:

$$2CuFeS_2 + 6H^+ + 2e^- \rightarrow Cu_2S + 2Fe^{2+} + 3H_2S \quad (16)$$

$$S^0 + 2H^+ + 2e^- \rightarrow H_2S \quad (17)$$

Peak 3:

$$2CuFeS_2 + 4H^+ + 2e^- \rightarrow Cu^0 + Fe^{2+} + 2H_2S \quad (18)$$

$$Cu_2S + 2H^+ + 2e^- \rightarrow 2Cu^0 + H_2S \quad (19)$$

Peak 4:

$$2Cu^0 + H_2S \rightarrow Cu_2S + 2H^+ + 2e^- \quad (20)$$

Peak 5 and Peak 6:

$$H_2S \rightarrow S^0 + 2H^+ + 2e^- \quad (21)$$

$$CuFeS_2 \rightarrow CuS + Fe^{2+} + S^0 + 2e^- \quad (22)$$

Peak 7:

$$Cu_2S \rightarrow Cu_xS + (2-x)Cu^{2+} + (4-2x)e^- \quad (23)$$

Peak 8:

$$CuFeS_2 \rightarrow Cu_{1-x}Fe_{1-y}S_{2-z} + xCu^{2+} + yFe^{2+} + zS^0 + 2(x+y)e^- \quad (24)$$

$$CuS \rightarrow Cu^{2+} + S^0 + 2e^- \quad (25)$$

$$2CuFeS_2 + 5H_2O \rightarrow 2CuO + Fe_2O_3 + 4S^0 + 10H^+ + 10e^- \quad (26)$$

Fig. 8a indicates that four peaks had appeared on the cyclic voltammograms of bornite. According to previous studies, peak a_1 corresponded to the equation (8-11), peak a_2 corresponded to the equation (17, 19, 27), peak a_3 corresponded to the equation (21) and peak a_4 corresponded to the equation (28-30) [17, 42].

$$3Cu_5FeS_4 + 6H^+ + 2e^- \rightarrow 5Cu_2S + 3H_2S + 2Fe^{2+} \quad (27)$$

$$Cu_5FeS_4 \rightarrow Cu_{5-x}FeS_4 + xCu^{2+} + 2xe^- \quad (28)$$

$$Cu_{5-x}FeS_4 + 6H^+ \rightarrow CuS + (4-x)Cu^{2+} + 3H_2S + Fe^{3+} + (5-2x)e^- \quad (29)$$

$$Cu_{5-x}FeS_4 \rightarrow (5-x)Cu^{2+} + Fe^{3+} + 4S^0 + (13-2x)e^- \quad (30)$$

According to previous studies, the chemical reactions of pyrite were simple. Fig. 8b indicates that the peaks on the cyclic voltammograms of pyrite were contained in the cyclic voltammograms of chalcopyrite-pyrite mixed ore.

Fig. 8a and Fig. 8b show that the cyclic voltammograms of chalcopyrite-bornite mixed ore and chalcopyrite-pyrite mixed ore contained all the anodic-cathodic reactions of sole chalcopyrite, bornite and pyrite, indicating that the electrochemical dissolution process of mineral in mixed ores did not change compared with that of sole mineral.

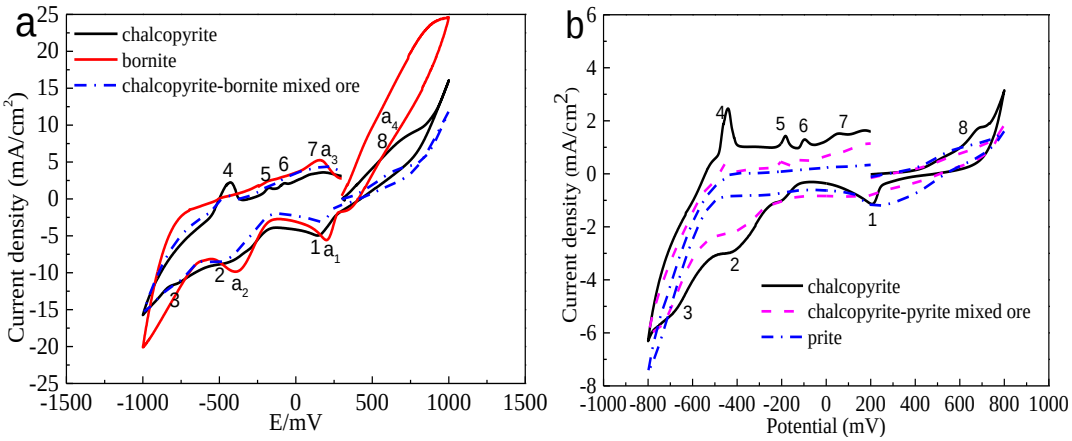

Figure 8. Cyclic voltammograms of chalcopyrite, bornite, pyrite, chalcopyrite-bornite mixed ore and chalcopyrite-pyrite mixed ore electrode.

3.5 A discussion on bioleaching mechanisms of mixed ores

According to the bioleaching results, it can be found that bioleaching behaviors of single chalcopyrite was significantly different compared with those of chalcopyrite-pyrite and chalcopyrite-bornite mixed ores. Real-time PCR technique showed that the change rules of percentages of *A.caldus* and *L.ferriphilum* during bioleaching were similar between bioleaching system of sole chalcopyrite and two kinds mixed ores, indicating that biological factor should not be the main cause for the different bioleaching behaviors. Electrochemical analysis showed that the electrochemical dissolution process of mineral in mixed ores did not change compared with that of sole mineral, indicating that the electrochemical interactions between each mineral did not significantly affect the different bioleaching behaviors. Hence, chemical factor should mainly account for the different bioleaching behaviors and copper extraction. Redox potential was widely considered as the determining factor in bioleaching [32, 43-47]. Combined with our previous researches, we further proposed that the redox potential in bioleaching systems of mixed ores was significantly different with that of single chalcopyrite, thus resulting in different bioleaching behaviors and copper extraction. In addition, we may try to control the redox potential at appropriate range by adjusting the percentages of different minerals to enhance chalcopyrite bioleaching.

4. CONCLUSIONS

Rodex potential analysis indicates that high copper extraction rate can be obtained when the solution potential was controlled within a suitable range (between E_L to E_H). In chalcopyrite-pyrite mixed ore bioleaching system, the redox potential can be maintained at the optimum potential interval in the presence of *A. caldus*. The results further proved that the optimum redox potential theory and the proposed mechanism of pyrite on chalcopyrite bioleaching were reliable.

In chalcopyrite-bornite mixed ore bioleaching system, the redox potential can be maintained at the optimum potential interval in the presence of *A. caldus* or *L. ferriphilum.* All of them can obtain high copper extraction rates. XRD and XPS analysis of chalcopyrite-bornite mixed type ore leached by *L. ferriphilum* for 10 days show that the S-containing materials on the surface of residues were mainly S^{2-}, S_2^{2-}, S^0 and SO_4^{2-}. No obvious Sn^{2-} was discovered in the leaching system. And a large amount of S^0 did not significantly impede the dissolution of chalcopyrite. The results further proved that the optimum redox potential theory and the proposed mechanism of bornite on chalcopyrite bioleaching were reliable.

Electrochemical anlaysis proved that the electrochemical dissolution processes of mixed ores and single chalcopyrite were similar, indicating that the electrochemical interactions between each mineral should not be the main cause for the different bioleaching behaviros and copper extractions.

Real-time PCR analysis proved that the percentage change rules of *A. caldus* and *L. ferriphilum* in the bioleaching systems of mixed ores and single chalcopyrite were similar, further indicating that the effect of pyrite and bornite on the bioleaching of chalcopyrite was mainly due to chemical factors, rather than biological factors.

ACKNOWLEDGEMENT
This work was supported by the National Natural Science Foundation of China (project No. 51704331 and No. 51320105006).

References

1. H. Zhao, X. Gan, J. Wang, L. Tao, W. Qin, and G. Qiu, *Hydrometallurgy*, 171 (2017) 374.
2. F. Anjum, M. Shahid, and A. Akcil, *Hydrometallurgy*, s 117–118 (2012) 1.
3. H.L. Ehrlich, *European Journal of Mineral Processing & Environmental Protectio*, (2004).
4. H. Zhao, J. Wang, X. Gan, X. Zheng, L. Tao, M. Hu, Y. Li, W. Qin, and G. Qiu, *Bioresource Technol.*, 194 (2015) 28.
5. N. Pradhan, K. C. Nathsarma, K. Srinivasa Rao, L. B. Sukla, and B. K. Mishra, *Miner. Eng.*, 21 (2008) 355.
6. J. Vilcáez, K. Suto, and C. Inoue, *Int. J. Miner. Process.*, 88 (2008) 37.
7. H. Zhao, J. Wang, C. Yang, M. Hu, X. Gan, L. Tao, W. Qin, and G. Qiu, *Hydrometallurgy*, 151 (2015) 141.
8. H. Zhao, X. Huang, J. Wang, Y. Li, R. Liao, X. Wang, X. Qiu, Y. Xiong, W. Qin, and G. Qiu, *Miner. Eng.*, 109 (2017) 153.
9. D.G. Dixon, K. Baxter, and L. Sylwestrzak, *Alta Copper*, 11 (2007).
10. D. Dixon, D. Mayne, and K. Baxter, *Can. Metall. Quart.*, 47 (2008) 327.
11. G. Nazari, D. Dixon, and D. Dreisinger, *Hydrometallurgy*, 105 (2011) 251.

12. G. Nazari, D. Dixon, and D. Dreisinger, *Hydrometallurgy*, 113 (2012) 122.
13. N. Hiroyoshi, H. Miki, T. Hirajima, and M. Taunekawa, *Hydrometallurgy*, 57 (2000) 31.
14. N. Hiroyoshi, H. Miki, T. Hirajima, and M. Taunekawa, *Hydrometallurgy*, 60 (2001) 185.
15. K. Third, R. Cord-Ruwisch, and H. Watling, *Biotechnol. bioeng.*, 78 (2002) 433.
16. A. Elsherief, *Miner. Eng.*, 15 (2002) 215.
17. H.B. Zhao, M. Hu, Y. Li, S. Zhu, W. Qin, G. Qiu, and J. Wang, *T. Nonfree. Metal. Soc.*, 25 (2015) 303.
18. G. Gu, K. Hu, X. Zhang, X. Xiong, and H. Yang, *Electrochimica Acta*, 103 (2013) 50.
19. W. Qin, C. Yang, S. Lai, J. Wang, K. Liu, and B. Zhang, *Bioresource Technol.*, 129 (2013) 200.
20. C. L. Liang, J. Xia, Y. Yang, Z. Nie, X. Zhao, L. Zheng, C. Ma, and Y. Zhao, *Hydrometallurgy*, 107 (2011) 13..
21. D. Majuste, V. Ciminelli, K. Osseo-Asare, M. Dantas, and R. Magalhaes-Paniago, *Hydrometallurgy*, 111 (2012) 114.
22. R.G. Acres, S.L. Harmer, and D.A. Beattie, *Int. J. Miner. Process.*, 94 (2010) 43.
23. D.E. Rawlings, and D.B. Johnson, *Microbiology*, 153 (2007) 315.
24. D.B. Johnson, and K.B. Hallberg, *Res. Microbiol.*, 154 (2003) 466.
25. R.B. Hawkes, P.D. Franzmann, and J.J. Plumb, *Hydrometallurgy*, 83 (2006) 229.
26. D.B. Johnson, *Hydrometallurgy*, 59 (2001) 147.
27. D.A. Shirley, *Phys. Rev. B*, 5 (1972) 4709.
28. C. Klauber, *Int. J. Miner. Process.*, 86 (2008) 1.
29. H. Watling, *Hydrometallurgy*, 140 (2013) 163.
30. Y. Li, N. Kawashima, J. Li, A. Chandra, and A. Gerson, *Adv. Colloid. Interfa.*, 197 (2013) 1.
31. E. Córdoba, J. Munoz, M. Blazquez, F. Gonzalez, and A. Ballester, *Hydrometallurgy*, 93 (2008) 88.
32. Å. Sandström, A. Shchukarev, and J. Paul, *Miner. Eng.*, 18 (2005) 505.
33. E. Córdoba, J. Munoz, M. Blazquez, F. Gonzalez, and A. Ballester, *Hydrometallurgy*, 93 (2008) 106.
34. K. Third, R. Cord-Ruwisch, and H. Watling, *Hydrometallurgy*, 57 (2000) 225.
35. M. Gericke, Y. Govender, and A. Pinches, *Hydrometallurgy*, 104 (2010) 414.
36. J. Petersen, and D.G. Dixon, *Hydrometallurgy*, 83 (2006) 40.
37. A. Ahmadi, M. Schaffie, Z. Manafi, and M. Ranjbar, *Hydrometallurgy*, 104 (2010) 99.
38. H. Zhao, J. Wang, X. Gan, X. Zheng, L. Tao, M. Hu, Y. Li, W. Qin, and G. Qiu, *Bioresource Technol.*, 194 (2015) 28.
39. H. Zhao, J. Wang, X. Gan, M. Hu, L. Tao, and G. Qiu, *Hydrometallurgy*, 164 (2016) 159.
40. H. Zhao, J. Wang, W. Qin, M. Hu, S. Zhu, and G. Qiu, *Miner. Eng.*, 71 (2015) 159.
41. H. Zhao, J. Wang, M. Hu, W. Qin, Y. Zhang, and G. Qiu, *Bioresource Technol.*, 149 (2013) 71.
42. H. Zhao, J. Wang, W. Qin, M. Hu, and G. Qiu, *Int. J. Electrochem. Sci.*, 10 (2015) 848.
43. M. Khoshkhoo, M. Dopson, A. Shchukarev, and Å. Sandström, *Hydrometallurgy*, 144-145 (2014) 7.
44. M. Lotfalian, M. Ranjbar, M.H. Fazaelipoor, M. Schaffie, and Z. Manafi, *Miner. Eng.*, 81 (2015) 52.
45. A.J.H. Janssen, S. Meijer, J. Bontsema, and G. Lettinga, *Biotechnol. bioeng.*, 60 (2015) 147.
46. E.M. Cordoba, J.A. Munoz, M.L. Blazquez, F. Gonzalez, and A. Ballester, *Hydrometallurgy*, 93 (2008) 106.
47. K.A. Third, R. Cord-Ruwisch, and H.R. Watling, *Biotechnol. bioeng.*, 78 (2002) 433.